Pergamon

Adv. Space Res. Vol. 14, No. 9, pp. (9)83–(9)87, 1994

0273–1177/94 $6.00 + 0.00

LATITUDINAL VARIATION OF MIDDLE ATMOSPHERIC DENSITY AND TEMPERATURE

P. A. T. Haris, T. D. Stevens, S. Maruvada and C. R. Philbrick

The Pennsylvania State University, Applied Research Laboratory, University Park, PA, U.S.A.

ABSTRACT

Profiles of the latitudinal distribution of middle atmospheric density and temperature have been obtained from a ground based remote sensing instrument. A two color Rayleigh/Raman lidar, built at Penn State University, was part of the LADIMAS (Latitudinal Distribution of Middle Atmospheric Structure) campaign. The goal was to measure density, temperature, and trace constituents from the troposphere to the thermosphere on a global scale. Measurements were taken from 70° North to 65° South latitude during a three month period between September 1991 and January 1992. The data provides a unique opportunity to study the latitudinal variations of the mean temperature and the variability in the atmospheric structure. Comparisons of the atmospheric conditions to models, such as the CIRA atmospheric model, were made to study the deviations.

INTRODUCTION

During the past couple of decades, there has been an increasing interest in monitoring and studying the structure and dynamics of the middle atmosphere /1,2/ using various techniques with varying accuracies and resolutions. A Rayleigh/Raman lidar system was constructed at Penn State University during 1990-1991. In July 1991, the lidar was installed in a standard shipping container, which was designed to serve as a field laboratory. The Penn State LAMP lidar was designed as a Rayleigh/Raman system with the goal of measuring density and temperature from altitudes of 0.5 km to 80 km, and concentrations of gases, nitrogen and water vapor from 0.5 km to 35 km and 5 km, respectively /3/. Between September 1991 and January 1992, the LAMP lidar partook in the LADIMAS campaign whose goal was to measure density, temperature, and trace constituents of the atmosphere over the latitudinal range 70° N to 65° S.

Satellite measurements, as well as rocket measurements from several sites, have provided the data which are the basis for the latitudinal dependence of the CIRA Atmospheric model. It is the intention of this paper to present temperature and density profiles from the Penn State LAMP (Laser Atmospheric Measurement Program) lidar system and compare them to the CIRA: 1986 /4/ and US Standard Atmospheric (USSA76) models /5/. Most measurements were taken on-board the German research vessel RV Polarstern. A description of the voyage and meteorological conditions, together with a description of the instrument and signal processing techniques, are presented.

INSTRUMENTATION

The instrument consists of five principal subsystems: transmitter, receiver, detector, data system, and safety system. Light is emitted from a Nd:YAG laser, at a pulse repetition rate of 20 Hz with 7 ns long pulses, providing approximately 600 mJ pulses in the visible (532 nm) and 250 mJ pulses in the ultraviolet (355 nm). The energy in each pulse is measured and recorded by the data system. The laser beam is expanded through a five power telescope and directed into the atmosphere on the

axis of the receiving telescope. The receiver consists a 16" classical Cassegrain telescope with several beam steering components. The detector box utilizes a unique shuttering system and six separate detector channels to detect both high and low altitude Rayleigh data, and nitrogen and water vapor Raman data. The high altitude signal is shuttered over the first 15 km to prevent saturation of photon counting PMT's. A high speed data acquisition system allows 15 m resolution in the lower altitudes and 75 m resolution in the higher altitudes and Raman channels.

SIGNAL PROCESSING

Temperature calculations from Rayleigh lidar data can be achieved by integrating down relative density profiles using the hydrostatic equation and ideal gas law. Combining these two equations and solving for temperature /6/ yields,

$$T(z_1) = \frac{T(z_2)\,\rho(z_2)}{\rho(z_1)} + \frac{M}{R}\int_{z_1}^{z_2} \frac{g(z)\,\rho(z)}{\rho(z_1)}\,dz. \qquad (1)$$

where R is the gas constant for dry air, $\rho(z)$ is the density at altitude z, g is the acceleration of gravity, P(z) is the pressure at altitude z, and M is the mean molecular weight of the atmosphere. All that is needed for the integration is a starting temperature which can be found in atmospheric models. By selecting the cutoff end of the signal at a point where it matches closely with the CIRA model, errors caused by inaccurate starting temperatures can be minimized. On average only a few kilometers of signal were sacrificed in order to gain greater temperature accuracies. By starting the temperature integration at a lower density error, less temperature error is propagated down the curve. This process assumes that the scattering profiles represents the pure molecular atmosphere and that there are no contributions from aerosols. After the Mt. Pinatubo volcano erupted, the aerosol contamination of the molecular profile rose to heights near 35 km.

Background was eliminated by subtracting the averaged high altitude end of the signal. In a few cases where the atmospheric signal was not of insignificant value, the tail end of the signal was fitted to the CIRA model /1/. Due to the shutter wheel configuration, there were only a few data points on the top end of the signal for which an average background could be calculated. Fluctuations in this value made it difficult to pin down an exact value. Background errors, N_B, can alter the temperature, $\Delta T(z_1)$, by the equation /7/,

$$\Delta T(z_1) = \frac{z_2}{H}\frac{T(z_1)}{N(z_1)}\Delta N_B. \qquad (2)$$

As the photon count approaches the background error, larger temperature errors are incurred. The larger photon counts in the lower altitudes are not effected as much.

It is difficult to draw comparisons to monthly and latitudinal mean temperatures with only a few hours of measured data. Significant fluctuations can be seen in 5 and 30 minute data samples from the effects of gravity wave propagation /8/. In order to average out any small scale wave structures, the data were height reduced to 1 km and integrated from 1 to 4.5 hours. Long integrations reduce the superposition of waves which could cause larger temperature fluctuations and deviations from the mean temperature. The raw data was then processed using a Hanning filter with a window size that increased with increasing altitude. The window has a minimum size of 2 km at 20 km altitude and a maximum size of 7.8 km at 70 km altitude.

OBSERVATIONS

During the METALS campaign at the Andoya Rocket Range, the LAMP lidar obtained data together with meteorological rockets. One of these comparisons is shown in Figure 1. The lidar data were integrated over 30 minutes and height reduced to 150 meters in order to closely match the rocket resolution. Both the 355 nm and 532 nm data channels follow the rocket measurements closely. The error bars signify only the statistical error due to the number of photon counts.

Figures 2, 3, and 4, show data from the two-color measurements of the LAMP lidar during the LADIMAS campaign. The solid lines signify the CIRA model. Figure 2 demonstrates close correlation of the LAMP data to the CIRA model. Temperature is extended down to 25 km, since the Pinatubo dust layer was not very prominent above the lower stratosphere in the high latitude regions. Increases in wave activity, shown in both Figures 3 and 4, cause noticeable deviations from the CIRA model.

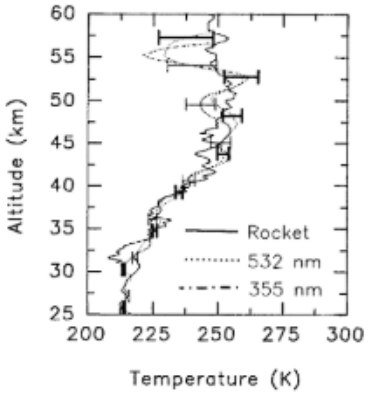

Figure 1. Comparison of Rocket and LAMP lidar data using 532 and 355 nm wavelengths. 11/04/91 0039 UT. 30 minute average.

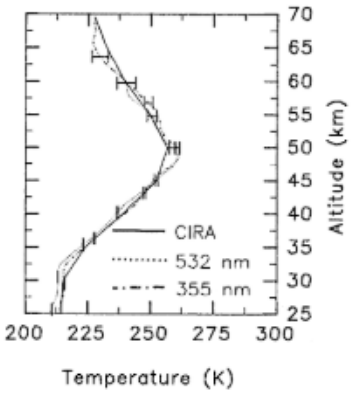

Figure 2. Comparison between CIRA: 1986 Atm. model and LAMP lidar data measured on 11/10/91 at 1712 - 1817 UT. 60 minute average.

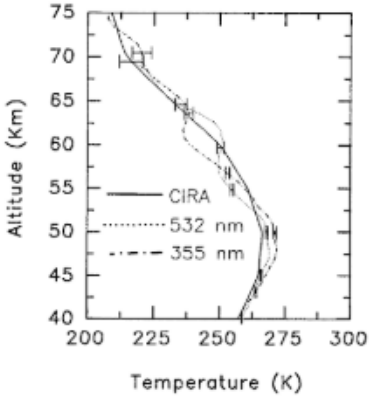

Figure 3. Comparison between CIRA: 1986 Atm. model and LAMP lidar data measured on 12/01/91 at 0026 - 0650 UT. 270 minute average.

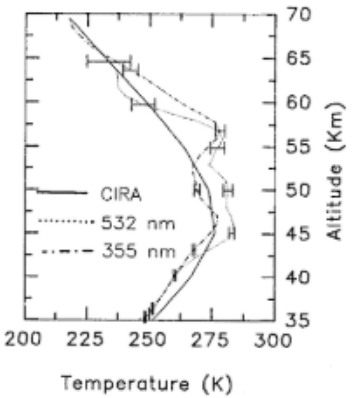

Figure 4. Comparison between CIRA: 1986 Atm. model and LAMP lidar data measured on 12/06/91 at 0455 - 0632 UT. 90 minute average.

Figure 5 provides a summary of density ratios and temperatures for the entire LADIMAS campaign over several height intervals. The solid lines are the CIRA model ratio, while the circles are the measured average signal ratio. Data from the LAMP lidar was selected at 10° latitude intervals, since the CIRA model gives temperature and pressure data at 10° latitude intervals. The density ratio plots were obtained by forming the ratio of the CIRA model and the LAMP signal to the USSA76 model. The ratios to the USSA76 model provide information about how well the CIRA model and the present measurements agree in distribution over latitude and month. At 35 km altitude, between 40° S and the equator, the Pinatubo aerosols contaminate the signal and thus have been removed from the plot. Above 40 km there are no effects from the stratospheric aerosol layer. Because of heavy cloud coverage, there are a few missing points at 60 km where the data did not achieve the limit of 4% statistical error. Seasonal changes in temperature and density are the main cause for the structure of the CIRA model over the latitudinal range of Figure 5. We have found that the density and temperature, measured by the LAMP lidar, follow the CIRA model closely in these altitude regions.

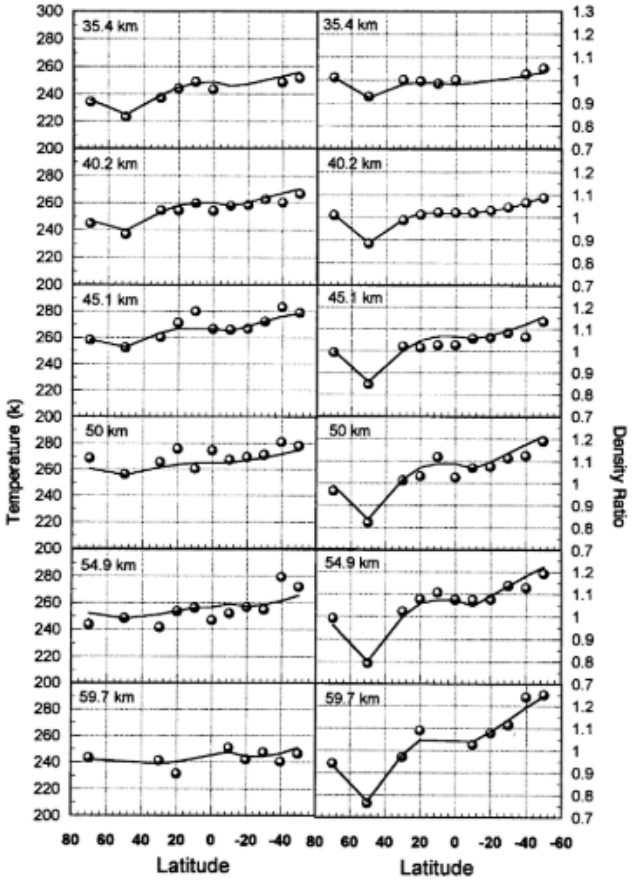

Figure 5. Temperature and density ratios for both LAMP data and the CIRA model as a function of latitude, season, and altitude.

CONCLUSIONS

The LAMP Lidar provided an enormous data base, which covers 70° N to 65° S latitude. There was a unique opportunity to compare our lidar results with established models, such as CIRA, which encompass the range of our data. We have found, in this preliminary analysis, that there is a high degree of correlation between our temperatures and densities and the CIRA temperatures and densities. The investigation has shown the impact of careful processing of data, which is absolutely necessary when analyzing Rayleigh data for density and temperature. Small errors in the density gradient will lead to very large errors in the temperature calculation. Great care must be taken, therefore, when subtracting the background, since so few signal counts exist at the higher altitudes.

ACKNOWLEDGMENTS

We would like to express our appreciation for support from NSF, the U.S. Navy's Environmental Systems Program Office, and the Pennsylvania State University's Applied Research Laboratory and College of Engineering. Participation in the LADIMAS campaign was made possible by the invitation of the Alfred-Wegener-Institute. Appreciation to several colleagues, particularly Professors U. von Zahn and D. Offermann, is gratefully acknowledged. The contributions made by D.B. Lysak, Yi-Chung Rau, and D.E. Upshaw are also greatly appreciated.

REFERENCES

1. M. L. Chanin, A. Hauchecorne, "LIDAR Studies of Temperature and Density Using Rayleigh Scattering," *MAP Handbook*, No. 13, 87 - 99, 1984.
2. C. R. Philbrick, "Measurements of Structural Features in Profiles of Mesospheric Density," *MAP Handbook*, 2, 333 - 340, 1981.
3. C. R. Philbrick, D. B. Lysak, T. D. Stevens, P. A. T. Haris, and Y. -C. Rau, "Atmospheric Measurements Using the LAMP Lidar During the LADIMAS Campaign," *Proc. of the 16th Inter. Laser Radar Confr.*, NASA Conference publications, No. 3158 , pp. 651 to 654, 1992.
4. COSPAR International Reference Atmosphere: 1986, Part II Middle Atmosphere Models, edited by D. Rees, J. J Barnett, K. Labitzke, Pergamon Press, Oxford, 1990.
5. U.S. Standard Atmosphere, 1976, National Oceanic and Atmospheric Administration, 1976.
6. C. R. Philbrick, F. J. Schmidlin, K. U. Grossmann, G. Lange, D. Offermann, K. D. Baker, D. Krankowsky, U. von Zahn, "Density and Temperature Structure Over Northern Europe," *J. of Atmos. and Terr. Phys.*, 47, 159 - 172, 1985.
7. L. T. Metzger, C. S. Gardner, "Temperature Determination from a Rayleigh Lidar," EOSL rep. #89-001, University of Illinois, 1989.
8. M. L. Chanin, A. Hauchecorne, "LIDAR Observations of Gravity and Tidal Waves in the Middle Atmosphere," *J. Geophys. Res.*, 86, 9715-9721, 1981.